

1 **Interhemispheric Influence of the Northern Summer Monsoons on the**
2 **Southern Subtropical Anticyclones**

3
4
5
6
7 Sang-Ki Lee^{1,2}, Carlos R. Mechoso³, Chunzai Wang², and J. David Neelin³

8 ¹Cooperative Institute for Marine and Atmospheric Studies, University of Miami, Miami FL

9 ²Atlantic Oceanographic and Meteorological Laboratory, NOAA, Miami FL

10 ³Department of Atmospheric and Oceanic Sciences, University of California, Los Angeles, Los
11 Angeles, CA

12
13
14
15
16
17
18 Revised and resubmitted to Journal of Climate (2nd revision)

19 July 2013

20
21
22 Corresponding author address: Dr. Sang-Ki Lee, NOAA/AOML, 4301 Rickenbacker Causeway,

23 Miami, FL 33149, USA. E-mail: Sang-Ki.Lee@noaa.gov.

1 **Abstract**

2 The southern subtropical anticyclones are notably stronger in the austral winter than in
3 summer particularly over the Atlantic and Indian Ocean basins. This is in contrast with the
4 Northern Hemisphere, in which subtropical anticyclones are more intense in summer according
5 to the “monsoon heating” paradigm. To better understand the winter intensification of southern
6 subtropical anticyclones, the present study explores the interhemispheric response to monsoon
7 heating in the northern hemisphere (NH) during the austral winter. A specially designed suite of
8 model experiments is performed in which summer monsoons in the NH are artificially
9 weakened. The highlight of our findings is that during the boreal summer enhanced tropical
10 convection activity in the NH plays crucial roles in either maintaining or strengthening the
11 southern subtropical anticyclones. Enhanced convection in the NH largely associated with the
12 major summer monsoons produces subsidence over the equatorial oceans and the tropical
13 southern hemisphere (SH) via an interhemispheric meridional overturning circulation and
14 increases the sea level pressure locally. In addition, suppressed convection over some regions of
15 subsidence produce stationary barotropic Rossby waves that propagate far beyond the tropics.
16 These stationary barotropic Rossby waves and those forced directly by the summer heating in the
17 NH are spatially phased to strengthen the southern subtropical anticyclones over all three oceans.
18 The interhemispheric response to the NH summer monsoons is most dramatic in the South
19 Pacific, where the subtropical anticyclone nearly disappears in the austral winter without the
20 influence from the NH.

1 **1. Introduction**

2 In our current understanding, the principal driver of the subtropical anticyclones (also known
3 as the subtropical highs) varies with season. The driver is heating associated with the monsoons
4 over the adjacent continents during the summer season, and orographic effects on the trade
5 easterlies and mid-latitude westerlies during the winter season (Rodwell and Hoskins 2001;
6 hereafter RH01). RH01 argued that the monsoon heating generates a Kelvin wave response over
7 the ocean to the east forming the equatorward portion of the subtropical anticyclone with a
8 poleward low-level jet to satisfy Sverdrup balance. The monsoon heating also generates a
9 Rossby wave response that produces adiabatic descent over the regions to the west (Rodwell and
10 Hoskins 1996). An equatorward low-level jet forms to satisfy Sverdrup balance closing off the
11 subtropical anticyclone on its eastern flank. Additional effects, such as intense near-surface
12 sensible heating over continents and air-sea interactions involving cold sea surface temperatures
13 (SSTs) and low-level clouds in the eastern part of the oceans, also contribute to drive the
14 subtropical anticyclones in the summer season (e.g., Seager et al. 2003; Liu et al. 2004;
15 Miyasaka and Nakamura 2005). In the winter season, monsoon heating is absent and the
16 subtropical anticyclones weaken. Consistent with this line of reasoning, the subtropical
17 anticyclones in the Northern Hemisphere (NH) are stronger and better defined in the boreal
18 summer than in winter (see Fig. 1 obtained with data from the NCEP-NCAR reanalysis). See
19 Ting (1994), Chen et al. (2001) and Chen (2003) for further discussions on the stationary wave
20 response to summer monsoon heating in the NH.

21 The subtropical anticyclones in the Southern Hemisphere (SH) show qualitatively different
22 behavior: They are notably stronger in the austral winter than in summer over the Atlantic and
23 Indian Ocean basins (see Fig. 1). This could be due to a combination of two effects: (1)

1 monsoons are less important in the mostly ocean-covered SH, and (2) topographic effects
2 become stronger in winter as the flow intensifies. The former is plausible because the
3 summertime subtropical anticyclones are significantly stronger in the NH than in the SH
4 (Miyasaka and Nakamura 2010). However, the latter is questionable because the circulation in
5 the SH has weaker seasonal variability. Furthermore, although the Andes cordillera is high and
6 has strong slopes, the topography over southern Africa and Australia is relatively low and has a
7 weaker blocking effect on the mean westerly flow (Richter and Mechoso 2004; 2006).

8 Some revision of the conceptual model of RH01 is, therefore, needed to address the
9 seasonality of the southern subtropical anticyclones. Recent studies with numerical models have
10 provided new insights on this issue. Wang et al. (2010) used an atmospheric general circulation
11 model (AGCM) to demonstrate that convection over the Western Hemisphere warm pool
12 (WHWP) during the boreal summer (austral winter) can produce adiabatic subsidence over the
13 southeastern tropical Pacific, and thus maintain the equatorward portion of the South Pacific
14 subtropical anticyclone and the equatorward low-level jet over the southeastern tropical Pacific.
15 In addition, Wang et al. (2010) showed, by performing experiments with the simple two-level
16 atmospheric model developed by Lee et al. (2009), that the interhemispheric connection between
17 the WHWP and the South Pacific subtropical anticyclone depends critically on the configuration
18 of the mean zonal winds in the SH. Richter et al. (2008) demonstrated a similar interhemispheric
19 connection between the African - Indian summer monsoon and the South Atlantic subtropical
20 anticyclone by comparing simulations by two versions of the University of California, Los
21 Angeles (UCLA) AGCM that reproduce climate features with significantly different success.

22 Based on the studies by Wang et al. (2010) and Richter et al. (2008) one could advance the
23 following conjecture: Interhemispheric teleconnections associated with the major summer

1 monsoons and deep tropical convection over warm SSTs in the NH contribute to the wintertime
2 strengthening of the southern subtropical anticyclones. The present study examines this
3 conjecture. Our goals are to explore to what extent the southern subtropical anticyclones during
4 the austral winter are affected by the major monsoons and deep tropical convection in the NH
5 and to gain insight on the underlying mechanisms at work for the teleconnections. To achieve
6 these goals we perform and analyze a suite of specially designed AGCM experiments
7 complemented by additional experiments using a simple atmosphere model.

8 In evaluating the subtropical anticyclone response we focus primarily on sea level pressure
9 (SLP). SLP will have contributions arising from both baroclinic and barotropic dynamics, and
10 can be made precise in models that carry out a vertical mode decomposition (e.g., Lee et al.
11 2009; Neelin and Zeng 2000). In these, the first baroclinic mode has high surface pressure and
12 cool tropospheric temperature in regions of upper-level convergence and adiabatic subsidence,
13 and low surface pressure and warm tropospheric temperature in regions of diabatic heating. The
14 baroclinic Rossby wave response to monsoon heating forms the basis of the Rodwell-Hoskins
15 mechanism, but can in turn excite barotropic Rossby waves via several interaction mechanisms:
16 vertical wind shear and surface stress acting on the baroclinic mode, and vertical advection of
17 baroclinic mode vorticity (e.g., Lee et al. 2009; Ji et al. 2013). The barotropic mode contribution
18 to subtropical SLP can thus have significantly different teleconnection characteristics than the
19 direct baroclinic mode contribution.

20 In section 2 we present our research strategy, give a brief description of the AGCM we use,
21 and list the AGCM experiments we performed. Next, using the AGCM results, we describe the
22 sea level pressure response in the SH over each ocean basin to the major summer monsoons in
23 the NH. In sections 4 and 5, we analyze the AGCM experiments to build a hypothesis that the

1 major summer monsoons in the NH force interhemispheric meridional overturning circulation,
2 and the diabatic cooling over certain sinking regions forces stationary barotropic Rossby waves
3 in the extratropical SH to enhance the southern subtropical anticyclones. In section 6, this
4 hypothesis is demonstrated by using the simple two-level model of Lee et al. (2009). In section
5 7, a summary and discussion is provided.

6

7 **2. Strategy, model, and experiments**

8 Our strategy is based on performing AGCM runs in which a control simulation (CTRL) is
9 compared to an idealized experiment with artificially weakened summer monsoons in the NH.
10 This weakening is achieved by synchronizing the seasonal cycles in the model's external and
11 boundary conditions across hemispheres, i.e., by shifting both the insolation at the top of the
12 atmosphere (TOA) and the SSTs and sea ice cover in the NH *only* by one-half the seasonal cycle
13 (6 months). Figure 2 shows the TOA solar insolation in the experiment (SYNC). In SYNC,
14 therefore, there is a global warm season in December-February (DJF) and a global cold season in
15 June-July (JJA), which correspond to those in the SH.

16 We use the NCAR Community Atmospheric Model version 4 (CAM4). CAM4 is a global
17 atmosphere-land model with prescribed SSTs and sea ice cover (Neale et al. 2012). The finite
18 volume dynamic core has a horizontal resolution of 2.5° (zonal) \times 1.9° (meridional) and 26
19 hybrid sigma-pressure layers. AGCM runs are 20-years long, of which the first five years are
20 discarded to exclude any possible transient spinup effects. The time mean of the remaining 15
21 years is analyzed in the following sections.

22

23 **3. Results**

1 Figure 3 shows the mean SLP obtained in CTRL for DJF and JJA. The simulated subtropical
2 anticyclones are realistic but generally stronger than in the NCEP-NCAR reanalysis (see Fig. 1).
3 The simulation captures two important features of the subtropical anticyclones: 1) those in the
4 NH are better defined in the boreal summer than in winter, and 2) those in the SH remain quite
5 strong and well defined in the austral winter. In view of these results, it is reasonable to conclude
6 that CAM4 is an appropriate tool for the present study.

7 Figure 4 shows time-latitude plots of monthly-mean, zonally averaged SLP over the South
8 Pacific, South Atlantic and South Indian Oceans from the NCEP-NCAR reanalysis, CTRL and
9 SYNC. The zonal average is carried out from the eastern to the western boundaries of the
10 respective ocean basin.

11 Starting with the South Pacific, the maximum SLPs in both the NCEP-NCAR reanalysis and
12 CTRL occur during the austral spring (August-November; Figs. 4a and d). In SYNC, however,
13 when the interhemispheric effect is removed, (Fig. 4g), the maximum SLPs occur in DJF and the
14 minimum in July - August. This feature of the seasonal cycle is consistent with the monsoon
15 heating mechanism of RH01. This suggests that the NH heating is a key contributor to the
16 strength of the subtropical anticyclone over the South Pacific during the austral winter.

17 For the South Atlantic and South Indian Oceans, the maximum SLPs in both the NCEP-
18 NCAR reanalysis and CTRL occur around July - August (Figs. 4b and e). In SYNC (Fig. 4h), the
19 maximum SLP occurs a little earlier with a much weaker magnitude than in CTRL (Fig. 4e).
20 This suggests again that the NH heating plays a major role in the strengthened subtropical
21 anticyclones over the South Atlantic and South Indian Oceans during the austral winter. It is
22 interesting to note that the maximum SLPs still do not occur in the austral summer, suggesting
23 that the subtropical anticyclones over the South Atlantic and South Indian Oceans could be still

1 strengthened during the austral winter without the NH heating. A potential mechanism that may
2 explain this seasonal cycle in SYNC is discussed in section 7.

3 In summary, the AGCM experiments indicate that the interhemispheric response to the NH
4 heating plays a crucial role in either maintaining or strengthening the southern subtropical
5 anticyclones in the austral winter. The interhemispheric response is very strong over all three
6 oceans, but it is more dramatic in the South Pacific because the subtropical anticyclone in this
7 ocean nearly disappears in the austral winter without the influence from the NH. In the following
8 sections we explore the physical processes that determine the interhemispheric response to the
9 heating in the NH and its impact on the southern subtropical anticyclones.

10

11 **4. Interhemispheric meridional overturning circulation**

12 In CTRL, the mean Hadley circulation during JJA (Fig. 5a) shows rising motion in the
13 tropical NH and sinking motion in the tropical SH. In SYNC, with external and boundary
14 forcings in the NH corresponding to DJF, this configuration changes drastically (Fig. 5b).
15 Instead, there is a pair of “Hadley cells” with rising motion near the thermal equator at around
16 5°N and sinking motion in the latitude band between 15° and 30° of each hemisphere. The
17 difference in the Hadley circulations between CTRL and SYNC (Fig. 5c) is the net meridional
18 overturning circulation forced by the NH heating during the warm season of that hemisphere.
19 The net interhemispheric meridional overturning circulation shown in Fig. 5c is, in general,
20 consistent with the suggestion on the association between the seasonal cycle of the Hadley cell
21 and the monsoons put forward by Dima and Wallace (2003).

22 Associated with the net interhemispheric meridional overturning circulation (Fig. 5c) is the
23 upper-level convergence field over the tropical SH. At the convergence centers subsiding air

1 tends to yield local SLP increases (e.g., Rodwell and Hoskins 1996). It is important to point out,
2 however, that the extent of the sinking branch of the net interhemispheric meridional overturning
3 circulation is limited to the deep tropics equatorward of around 20°S (Fig. 5c). Therefore, the
4 strengthening of the southern subtropical anticyclones south of around 20°S cannot be explained
5 as the direct result of the net interhemispheric meridional overturning circulation forced from the
6 NH.

7 Figure 6 shows the mean velocity potential and divergent winds during JJA at 200 hPa for
8 CTRL, SYNC and CTRL - SYNC. In CTRL, divergent winds (rising motions) occur over India
9 and East Asia, in association with the local summer monsoon, the northwestern tropical Pacific,
10 and the WHWP, whereas convergent winds (sinking motions) occur over the southeastern
11 tropical Pacific and much of the Atlantic especially the tropical South Atlantic (Fig. 6a). When
12 the interhemispheric effect is removed (i.e. SYNC), the centers of rising motion in the NH are
13 shifted toward the equator over the western equatorial Atlantic Ocean and the equatorial Indian
14 Ocean (Fig. 6b). Therefore, the net result of the interhemispheric response to the heating in the
15 NH is to produce subsidence over the western equatorial Atlantic Ocean and the equatorial
16 Indian Ocean (Fig. 6c).

17 In addition, a broad region of subsidence exists in CTRL – SYNC over the south-central
18 tropical Pacific, the southeastern tropical Pacific, and the tropical South Atlantic. It appears that
19 the subsidence in the south-central tropical Pacific is linked mainly to the summer expansion of
20 the western Pacific warm pool in the region of the northwestern tropical Pacific. The subsidence
21 in the southeastern tropical Pacific appears to be linked to the WHWP consistent with Wang et
22 al. (2010), whereas the subsidence over the tropical South Atlantic appears to be linked to the
23 Indian and West African summer monsoons, as suggested by Richter et al. (2008), and also to

1 the WHWP. These effects occur essentially as baroclinic mode teleconnections, which have no
2 trouble crossing the equator, but tend to remain trapped within the equatorial wave guide (Gill
3 1980). In the next two sections, we turn to potential barotropic contributions.

4

5 **5. Propagation of stationary Rossby waves to the subtropics**

6 As shown in Fig. 7a, the interhemispheric effect on SLP is not limited to the tropical SH
7 where the sinking branch of the net interhemispheric meridional overturning circulation directly
8 increases the local SLPs. Over the regions of subsidence in the equatorial oceans and the tropical
9 SH, slowly sinking air is heated by adiabatic compression and thus limits the vertical
10 development of convection. Therefore, the sinking regions in the south-central Pacific Ocean, the
11 western equatorial Atlantic Ocean, and the equatorial Indian Ocean are characterized by
12 suppressed moist convective heating rate at 500 hPa (Figure 8) and reduced convective
13 precipitation rate (not shown). Potentially, the diabatic cooling (i.e., reduced diabatic heating
14 relative to SYNC) over these regions can produce stationary barotropic Rossby waves far beyond
15 the tropics (e.g., Hoskins and Karoly 1981; Horel and Wallace 1981; Branstator 1983;
16 Sardeshmukh and Hoskins 1988; Ting and Held 1990; Lee et al. 2009). Consistent with this
17 hypothesis, the spatial pattern of SLPs in response to the interhemispheric teleconnections
18 closely resembles the stream function response at 500 hPa, which is a widely used proxy to
19 identify stationary barotropic Rossby waves (Fig. 7b). Note that the stream function sign is
20 reversed (i.e., circulation is anticlockwise around positive stream function) for a better visual
21 comparison with the SLP (Fig. 7a). It is important to point out that due to cold SSTs and low
22 level clouds, conditions are not suitable for deep convection in the southeastern tropical Pacific
23 or the southeastern tropical Atlantic. Therefore, the subsidence in these regions directly increases

1 the SLPs locally, but cannot induce diabatic cooling (Fig. 8) or force stationary barotropic
2 Rossby waves to the extratropical SH.

3

4 **6. Simple model experiments**

5 We next qualitatively examine the interpretation we have given to the differences between
6 CTRL and SYNC, particularly to the forcing of stationary barotropic Rossby waves shown in
7 Fig. 7b by diabatic cooling (i.e., reduced diabatic heating relative to SYNC) in the equatorial
8 oceans and the tropical SH. For such examination we select the simple atmospheric model of Lee
9 et al. (2009). This is a two-level, minimal complexity model of both the local and remote
10 stationary responses of the atmosphere to tropical heating anomalies. The model equations are
11 linearized about background wind fields, and recast as baroclinic and barotropic components
12 with thermal advection in the tropics neglected. See Lee et al. (2009) and Wang et al. (2010) for
13 more details about this model.

14 The band of easterlies in the tropics makes it difficult for stationary Rossby waves to
15 propagate across the equator (e.g., Branstator 1983). This is particularly true if the stationary
16 barotropic Rossby waves are forced in the tropical NH during the boreal summer when the zonal
17 background barotropic flow is mainly westward equatorward of around 20°N (Pexoto and Oort
18 1992). In the simple model experiments of Wang et al (2010), however, diabatic heating in the
19 tropical NH directly influences the SH without invoking the associated diabatic cooling. In Wang
20 et al. (2010), the baroclinic response to diabatic heating in the tropical NH comprises two centers
21 of low SLP anomalies, one in the northwest and the other in the southwest of the forcing region,
22 consistent with the simple Gill model (Matsuno 1966; Gill 1980). As further investigated by Ji et
23 al. (2013), the low SLP anomaly southwest of the forcing region in the tropical NH can be

1 positioned in the tropical SH with a weaker amplitude compared to its counterpart in the NH.
2 Also according to Ji et al. (2013), the Gill-type baroclinic circulations in the tropical SH may in
3 turn interact with the background flows in this hemisphere to produce stationary barotropic
4 Rossby waves.

5 Additionally, Watterson and Schneider (1987) suggested that a meridional background wind
6 associated with the Hadley circulation could enable wave propagation across the equator even
7 under an easterly background wind. Dima et al. (2005) analyzed the NCEP-NCAR reanalysis to
8 find some supporting evidences. Kraucunas and Hartmann (2007), and Liu and Wang (2013)
9 further demonstrated this mechanism using a nonlinear shallow-water model, and a linearized
10 simple two-level model, respectively.

11 An important implication drawn from the above-mentioned studies is that summertime
12 diabatic heating in the tropical NH can directly force stationary barotropic Rossby waves in the
13 extratropical SH, without invoking the associated diabatic cooling in the equatorial oceans and
14 the tropical SH, and thus can directly affect the southern subtropical anticyclones. Therefore, it is
15 important to address how effectively the diabatic heating in the tropical NH can directly induce
16 stationary barotropic Rossby waves in the extratropical SH.

17 In order to address these issues and also to further explore how the heating in the tropical NH
18 and the cooling in the equatorial oceans and the tropical SH considered separately in six major
19 forcing regions (see Fig. 8) affect the southern subtropical anticyclones, we performed seven
20 experiments using the simple two-level model. In the first experiment, the moist convective
21 heating rate at 500 hPa for JJA obtained from CTRL – SYNC (Fig. 8) is prescribed. The other
22 six experiments are identical to the first, except that the thermal forcing is prescribed only over
23 specified regions (see Fig. 8). In the second, third and fourth experiments, the moist convective

1 heating rate is prescribed only in the south-central Pacific ($150^{\circ}\text{E} - 130^{\circ}\text{W}$ and $20^{\circ}\text{S} - 5^{\circ}\text{N}$), the
2 western equatorial Atlantic ($60^{\circ}\text{W} - 10^{\circ}\text{W}$ and $10^{\circ}\text{S} - 7.5^{\circ}\text{N}$), and the equatorial Indian Ocean
3 ($60^{\circ}\text{E} - 110^{\circ}\text{W}$ and $20^{\circ}\text{S} - 10^{\circ}\text{N}$), respectively. In the rest of the three experiments, the moist
4 convective heating rate is prescribed only in the northwestern Pacific Ocean affected by summer
5 expansion of the western Pacific warm pool ($110^{\circ}\text{E} - 160^{\circ}\text{W}$ and $5^{\circ}\text{N} - 30^{\circ}\text{N}$), the WHWP
6 ($100^{\circ}\text{W} - 60^{\circ}\text{W}$ and $5^{\circ}\text{N} - 20^{\circ}\text{N}$), and the Indian summer monsoon region ($20^{\circ}\text{W} - 110^{\circ}\text{E}$ and
7 $10^{\circ}\text{N} - 30^{\circ}\text{N}$), respectively. See Fig. 8 for the regions of forcing and the heating rates prescribed
8 for these experiments.

9 For all seven experiments, the background fields are the zonally averaged climatological
10 stream function and velocity potential for JJA in the upper and lower troposphere derived from
11 CTRL. The simple two-level model assumes that barotropic divergence is zero (Lee et al. 2009).
12 Thus, the model is prescribed with only the baroclinic background velocity potential, which is
13 directly related to the Hadley cell in CTRL (Fig. 5a), and with both the barotropic and baroclinic
14 background stream functions. The zonally averaged barotropic and baroclinic background zonal
15 winds and the zonally averaged baroclinic meridional winds (computed from the stream function
16 and velocity potential fields) derived from SYNC and CTRL are shown in Fig. 9 along with
17 those derived from the NCEP-NCAR reanalysis. Since the simple model mainly solves a set of
18 linearized equations, nonlinear effects are not considered in our experiments.

19 Figure 10 shows the barotropic stream function response to the thermal forcing shown in Fig.
20 8. The stream function sign is again reversed (i.e., circulation is anticlockwise around positive
21 stream function) for a better visual comparison with the SLP in the AGCM experiments (Fig.
22 7a). The simple two-level model is an oversimplification of the real atmosphere, and is unable to
23 reproduce the exact shape or propagation pathway of the stationary Rossby waves simulated by

1 CAM4 (Fig. 7b). Nevertheless, a comparison between Figs. 7b and 10 reveals several important
2 common features. In particular, the anticyclones are roughly in place to enhance the southern
3 subtropical anticyclones in all three oceans.

4 Figure 11a, b and c show the barotropic stream function response to diabatic cooling in the
5 south-central Pacific Ocean, the western equatorial Atlantic Ocean, and the equatorial Indian
6 Ocean, respectively. It is clear that the stationary barotropic Rossby waves originating from the
7 south-central Pacific greatly strengthen the South Pacific subtropical anticyclone. Similarly, the
8 stationary barotropic Rossby waves originating from the western equatorial Atlantic Ocean
9 propagate to the extratropical South Atlantic and strengthen the South Atlantic subtropical
10 anticyclone. It appears that diabatic cooling in the equatorial Indian Ocean and the associated
11 stationary waves contribute to the strength of the South Indian subtropical anticyclone
12 particularly to the south and west of Australia.

13 Figure 12a, b and c show the barotropic stream function response to diabatic heating in the
14 northwestern Pacific Ocean, the WHWP, and the Indian summer monsoon region, respectively.
15 Unlike those forced in the south-central Pacific Ocean, the stationary barotropic Rossby waves
16 forced in the northwestern Pacific Ocean hardly influence the southern subtropical anticyclones.
17 The stationary waves directly forced in the WHWP only weakly influence the South Pacific
18 subtropical anticyclone.

19 However, it is interesting to note that the stationary waves directly forced in the Indian
20 summer monsoon region have large influences on the South Pacific and South Atlantic
21 subtropical anticyclones. This experiment is repeated without the baroclinic background
22 meridional winds to find that the baroclinic background meridional winds across the equator
23 (i.e., interhemispheric overturning circulation) play an important role in enhancing the

1 propagation of the Indian summer monsoon-forced stationary waves to the SH, in line with the
2 explanation offered by Watterson and Schneider (1987).

3 In summary, the simple model experiments support our hypothesis that, in response to the
4 heating in the tropical NH, diabatic cooling occurs in the equatorial oceans and the tropical SH,
5 and the cooling in the equatorial oceans and the tropical SH in turn force the stationary
6 barotropic Rossby waves shown in Fig. 7b, and thus strengthens the southern subtropical
7 anticyclones. The simple model experiments suggest that diabatic heating in the Indian summer
8 monsoon region can also enhance the South Pacific and South Atlantic subtropical anticyclones
9 without invoking the cooling in the equatorial oceans and the tropical SH.

10 In interpreting these barotropic Rossby wave trains, it should be recalled that they are excited
11 in the simple model by the specified diabatic heating or cooling (see Lee et al. 2009). The
12 diabatic cooling is itself a teleconnected response to heating in the tropical NH and is primarily a
13 reduction in deep convective heating that could potentially occur in certain locations over the
14 equatorial oceans and the tropical SH if the tropical NH heating were absent. It is also important
15 to recall that the simple two-level model does not include moist processes. Therefore, unless
16 prescribed, the simple model cannot simulate diabatic processes such as radiative cooling or
17 convective heating. See an intermediate complexity model study by Ji et al. (2013) for further
18 discussions on interhemispheric teleconnections in response to a localized heat source in the
19 tropical NH via the baroclinic mode affecting moist processes and thus convective heating in the
20 tropical SH.

21

22 **7. Summary and discussions**

1 The present study examines the conjecture that major summer monsoons in the NH
2 contribute to the wintertime strengthening of the southern subtropical anticyclones through
3 interhemispheric teleconnections. To explore this conjecture, we perform a specially designed
4 suite of AGCM experiment in which summer monsoons in the NH are artificially weakened. To
5 elucidate the underlying mechanisms at work for the teleconnections we also perform several
6 experiments using the simple numerical two-level model of Lee et al. (2009).

7 The results obtained in the AGCM and simple model experiments suggest that the
8 interhemispheric response to the heating in the NH does play a crucial role in either maintaining
9 or strengthening the southern subtropical anticyclones in the austral winter. Although the
10 interhemispheric response is very strong over all three oceans, it is more dramatic in the South
11 Pacific since subtropical anticyclone over this ocean nearly disappears in the austral winter
12 without the influence from the NH.

13 The sketch in Figure 13 summarizes the physical processes linking the major summer
14 monsoons in the NH and the southern subtropical anticyclones, encapsulating results from
15 several parts in the text. During the boreal summer, the interhemispheric meridional overturning
16 circulation is fueled from three hot spots in the tropical NH. These spots are located over the
17 Indian - East Asian summer monsoon region, the northwestern tropical Pacific region affected by
18 summer expansion of the western Pacific warm pool, and the WHWP (see Fig. 6). The
19 associated subsidence and SLP increases occur over the western equatorial Atlantic Ocean, the
20 equatorial Indian Ocean, the south-central tropical Pacific Ocean, the southeastern tropical
21 Pacific Ocean, and the South Atlantic Ocean. Since conditions are suitable for deep convection
22 in the western equatorial Atlantic Ocean, the equatorial Indian Ocean, and the south-central
23 tropical Pacific Ocean due to warm SSTs therein, the subsidence over these three regions

1 suppresses convection (see Fig. 8). The diabatic cooling (i.e., reduced diabatic heating relative to
2 SYNC) in these regions produces stationary barotropic Rossby waves that propagate far beyond
3 the tropical SH. These stationary Rossby waves and those forced directly by the summer heating
4 in the tropical NH are spatially phased to strengthen the southern subtropical anticyclones over
5 all three oceans.

6 It is argued that the stationary barotropic Rossby waves forced directly by the heating in the
7 tropical NH have a generally weaker influence on the southern subtropical anticyclones than
8 those forced by the cooling in the equatorial oceans and the tropical SH. However, the simple
9 two-level model used to arrive at that conclusion excludes nonlinear effects. Therefore, further
10 analyses are needed to clarify this point. A potentially promising method is to prescribe localized
11 heating profiles in a fully nonlinear AGCM (e.g., Jang and Strauss, 2012).

12 It is worthwhile to point out that the subtropical anticyclones over the South Atlantic and
13 South Indian Oceans could be still strengthened during the austral winter without the NH heating
14 (Fig. 4h and i). It appears that in the absence of the NH heating the equatorial oceans, especially
15 the equatorial Indian Ocean, could drive rising motions aloft to force subsidence motions over
16 the broad regions of South Atlantic and southwestern Indian Ocean (see Fig. 6b), and thus
17 increase SLPs therein.

18 Results of this study leave open some important scientific questions, which deserve future
19 investigations. For instance, in our AGCM experiments the model SSTs in the SH are not
20 allowed to respond to (or to the lack of) the interhemispheric teleconnections. Therefore, it
21 remains to be determined if and how our conclusions are modified if thermal and dynamic
22 interactions with the surface ocean mixed layer are activated. An important and related point is
23 that the trade winds over the SH are closely linked to the southern subtropical anticyclones. An

1 enhanced southern subtropical anticyclone during the boreal summer could potentially increase
2 the trade winds in the SH, and thus affect surface ocean dynamics and SSTs in the tropical SH.
3 To explore potential air-sea interactions involving the interhemispheric teleconnections, the next
4 step is to perform experiments of the CTRL and SYNC type with CAM4 coupled to a slab ocean
5 mixed layer model over the SH.

6

7 **Acknowledgments.** We would like to thank three anonymous reviewers for their thoughtful
8 comments and suggestions, which led to a significant improvement of the paper. We also would
9 like to thank Teresa Losada, Xiao Heng, and Xuan Ji for their helpful comments and
10 contributions through our science discussions between the University of Miami and UCLA, and
11 Marlos Goes and George Halliwell for their useful comments and suggestions. This work was
12 supported by grants from the National Science Foundation (NSF) and the National Oceanic and
13 Atmospheric Administration (NOAA)'s Climate Program Office, and by the base funding of
14 NOAA Atlantic Oceanographic and Meteorological Laboratory (AOML).

15

16

REFERENCES

- 17 Branstator, G., 1983: Horizontal energy propagation in a barotropic atmosphere with meridional
18 and zonal structure. *J. Atmos. Sci.*, **40**, 1689–1708.
- 19 Chen, P., M. P. Hoerling, and R. M. Dole, 2001: The origin of the subtropical anticyclones. *J.*
20 *Atmos. Sci.*, **58**, 1827–1835.
- 21 Chen, T.-C., 2003: Maintenance of summer monsoon circulations: A planetary-scale perspective.
22 *J. Climate*, **16**, 2022–2037.

1 Dima, I. M., and J. M. Wallace, 2003: On the seasonality of the Hadley cell. *J. Atmos. Sci.*, **60**,
2 1522-1527.

3 Dima, I. M., J. M. Wallace, I. Kraucunas, 2005: Tropical zonal momentum balance in the NCEP
4 reanalyses. *J. Atmos. Sci.*, **62**, 2499-2513.

5 Gill, A. E., 1980: Some simple solutions for heat-induced tropical circulation. *Quart. J. Roy.*
6 *Meteor. Soc.*, **106**, 447-462.

7 Horel, J. D., and J. M. Wallace, 1981: Planetary-scale atmospheric phenomena associated with
8 the Southern Oscillation. *Mon. Wea. Rev.*, **109**, 813-829.

9 Hoskins, B. J., and D. J. Karoly, 1981: The steady linear response of a spherical atmosphere to
10 thermal and orographic forcing. *J. Atmos. Sci.*, **38**, 1179-1196.

11 Jang, Y., D. M. Straus, 2012: The Indian monsoon circulation response to El Niño diabatic
12 heating. *J. Climate*, **25**, 7487-7508.

13 Ji, X., J. D. Neelin, S.-K. Lee, and C. R. Mechoso, 2013: Interhemispheric teleconnections from
14 tropical heat sources in intermediate and simple models. *J. Climate*, in-revision.

15 Kraucunas, I., and D. L. Hartmann, 2007: Tropical stationary waves in a nonlinear shallow-
16 water model with realistic basic states. *J. Atmos. Sci.*, **64**, 2540-2557.

17 Lee, S.-K., C. Wang, and B. Mapes, 2009: A simple atmospheric model of the local and
18 teleconnection responses to heating anomalies. *J. Climate*, **22**, 272-284.

19 Liu, F., and B. Wang, 2013: Mechanisms of global teleconnections associated with the Asian
20 summer monsoon: An intermediate model analysis. *J. Climate*, **26**, 1791-1806.

21 Liu, Y. M., G. X. Wu, and R. Ren, 2004: Relationship between the subtropical anticyclone and
22 diabatic heating. *J. Climate*, **17**, 682-698.

- 1 Matsuno, T., 1966: Quasi-geostrophic motions in the equatorial area. *J. Meteor. Soc. Japan*, **44**,
2 25–43.
- 3 Miyasaka, T., and H. Nakamura, 2005: Structure and formation mechanisms of the Northern
4 Hemisphere summertime subtropical highs. *J. Climate*, **18**, 5046–5065.
- 5 Miyasaka, T., and H. Nakamura, 2010: Structure and mechanisms of the Southern Hemisphere
6 summertime subtropical anticyclones. *J. Climate*, **23**, 2115–2130.
- 7 Neale, R. B., J. Richter, S. Park, P. H. Lauritzen, S. J. Vavrus, P. J. Rasch, and M. Zhang, 2012:
8 The mean climate of the community atmosphere model (CAM4) in forced SST and fully
9 coupled experiments. *J. Climate*, submitted.
- 10 Neelin, J. D., and N. Zeng, 2000: A quasi-equilibrium tropical circulation model – formulation.
11 *J. Atmos. Sci.*, **57**, 1741-1766.
- 12 Peixoto, J. P., and A. H. Oort, 1992: *Physics of Climate*. American Institute of Physics, 520 pp.
- 13 Richter, I., and C. R. Mechoso, 2004: Orographic influences on the annual cycle of Namibian
14 stratocumulus clouds. *Geophys. Res. Lett.*, **31**, L24108.
- 15 Richter, I. and C. R. Mechoso, 2006: Orographic influences on subtropical stratocumulus. *J.*
16 *Atmos. Sci.*, **63**, 2585-2601.
- 17 Richter, I., C. R. Mechoso, and A. W. Robertson, 2008: What determines the position and
18 intensity of the South Atlantic anticyclone in austral winter? - An AGCM study. *J. Climate*,
19 **21**, 214–229.
- 20 Rodwell, M. J., and B. J. Hoskins, 1996: Monsoons and the dynamics of deserts. *Q. J. Roy.*
21 *Meteorol. Soc.*, **122**, 1385-1404.
- 22 Rodwell, M. J., and B. J. Hoskins, 2001: Subtropical anticyclones and summer monsoons. *J.*
23 *Climate*, **14**, 3192-3211.

1 Sardeshmukh, P. D., and B. J. Hoskins, 1988: The generation of global rotational flow by steady
2 idealized tropical divergence. *J. Atmos. Sci.*, **45**, 1228–1251.

3 Seager, R., R. Murtugudde, N. Naik, A. Clement, N. Gordon, and J. Miller, 2003: Air sea
4 interaction and the seasonal cycle of the subtropical anticyclones. *J. Climate*, **16**, 1948-1966.

5 Ting, M., and I. M. Held, 1990: The stationary wave response to tropical SST anomaly in an
6 idealized GCM. *J. Atmos. Sci.*, **47**, 2546–2566.

7 Ting, M., 1994: Maintenance of northern summer stationary waves in a GCM. *J. Atmos. Sci.*, **51**,
8 3286–3308.

9 Wang, C., S.-K. Lee, and C. R. Mechoso, 2010: Interhemispheric influence of the Atlantic warm
10 pool on the southeastern Pacific. *J. Climate*, **23**, 404-418.

11 Watterson, I. G., and E. K. Schneider, 1987: The effect of the Hadley Circulation on the meridional propagation of
12 stationary waves. *Q. J. Roy. Meteor. Soc.*, **13**, 779–813.

13

14

15

16

17 **Figure captions:**

18

19 Figure 1. Climatological sea level pressure for (a) DJF and (JJA) during 1971 - 2000 obtained
20 from the NCEP-NCAR Reanalysis. The unit is hPa.

21

22 Figure 2. Daily solar insolation at the top of the atmosphere in (a) CTRL, and (b) SYNC, and (c)
23 CTRL – SYNC. The unit is $W m^{-2}$.

1
2 Figure 3. Climatological sea level pressure for (a) DJF and (JJA) obtained from CTRL. The unit
3 is hPa.

4
5 Figure 4. Sea level pressure averaged zonally for (a, d, and g) the South Pacific Ocean, (b, e, and
6 h) the South Atlantic Ocean, and (c, f, and i) South Indian Ocean, obtained from (a, b and c) the
7 NCEP-NCAR reanalysis, (d, e and f) CTRL, and (g, h and i) SYNC. The unit is hPa.

8
9 Figure 5. Meridional overturning circulation (mass stream function) obtained from (a) CTRL, (b)
10 SYNC, and (c) CTRL – SYNC. Circulation is clockwise (anticlockwise) around positive
11 (negative) stream function. The unit is 10^9 Kg s^{-1} .

12
13 Figure 6. Velocity potential and divergent wind vector at 200 hPa obtained from (a) CTRL, (b)
14 SYNC, and (c) CTRL - SYNC. The units are $10^7 \text{ m}^2 \text{ s}^{-1}$ for velocity potential, and m s^{-1} for
15 divergent wind vector.

16
17 Figure 7. (a) Sea level pressure, (b) stream function and wind vector at 500 hPa obtained from
18 CTRL - SYNC. The zonal line at 40°S roughly marks the southern end of the southern
19 subtropical anticyclones in JJA. The stream function sign is reversed in such a way that
20 circulation is anticlockwise around positive stream function. The units are hPa for sea level
21 pressure, $10^7 \text{ m}^2 \text{ s}^{-1}$ for stream function, and m s^{-1} for wind vector.

22

1 Figure 8. Moist convective heating rate at 500 hPa in JJA obtained from CTRL - SYNC. The
2 unit is K day^{-1} . The three regions of diabatic heating in the NH, namely the northwestern Pacific
3 Ocean affected by summer expansion of the western Pacific warm pool, the, and the Indian
4 summer monsoon region are indicated by red borderlines. The three regions of diabatic cooling
5 in the equatorial oceans and the tropical SH, namely the south-central Pacific, the western
6 equatorial Atlantic, and the equatorial Indian Ocean are shown with blue borderlines.

7

8 Figure 9. Zonally averaged climatological (a) barotropic zonal, (b) baroclinic zonal and (c)
9 baroclinic meridional winds in JJA obtained from SYNC (solid lines), CTRL (long-dashed lines)
10 and the NCEP-NCAR reanalysis (short-dashed line). The barotropic zonal winds are obtained by
11 vertically averaging the zonal winds in the troposphere (100 ~ 1000 hPa). To compute the
12 baroclinic zonal winds, the zonal winds are vertically averaged separately for the upper
13 troposphere (100 ~ 500 hPa) and for the lower troposphere (500 ~ 1000 hPa), and the latter is
14 subtracted from the former then divided by 2. The same methodology is used to compute the
15 baroclinic meridional winds.

16

17 Figure 10. Barotropic stream function and wind vector responses in the simple model
18 experiments to the moist convective heating and cooling derived from CTRL – SYNC. The units
19 are $10^7 \text{ m}^2 \text{ s}^{-1}$ for stream function, and m s^{-1} for wind vector.

20

21 Figure 11. Barotropic stream function and wind vector responses in the simple model
22 experiments to diabatic cooling in (a) the central South Pacific Ocean, (b) the western equatorial

1 Atlantic Ocean, and (c) the equatorial Indian Ocean. The units are $10^7 \text{ m}^2 \text{ s}^{-1}$ for stream function,
2 and m s^{-1} for wind vector.

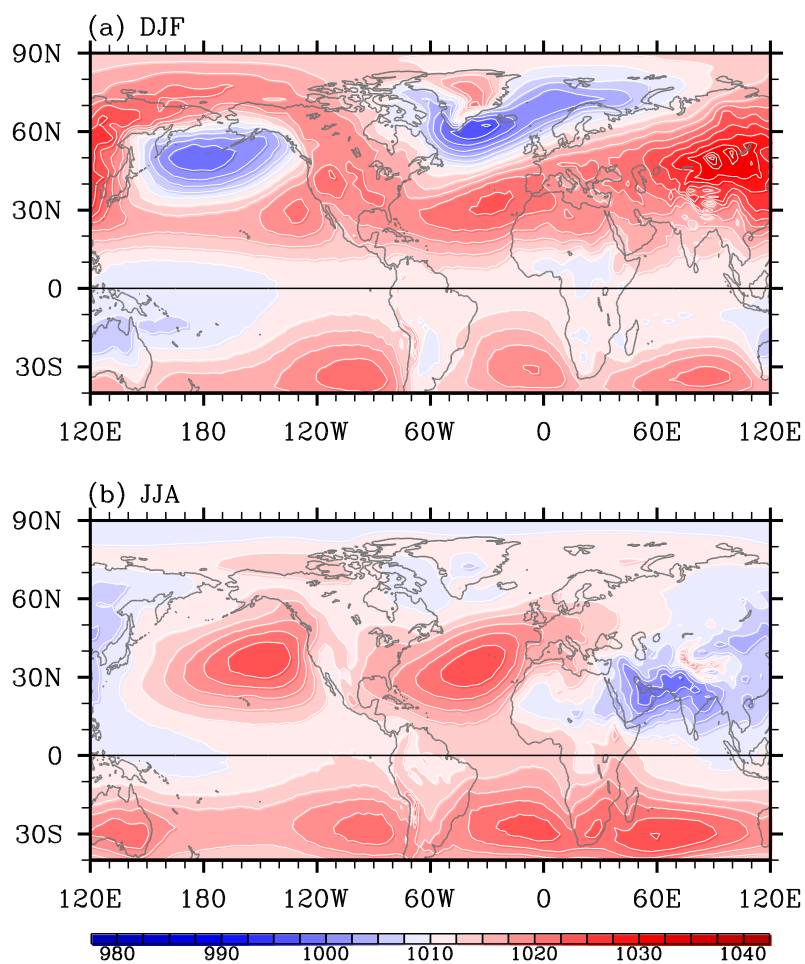
3

4 Figure 12. Barotropic stream function and wind vector responses in the simple model
5 experiments to diabatic heating in (a) the northwestern Pacific Ocean, (b) the WHWP, and (c)
6 the Indian summer monsoon region. The units are $10^7 \text{ m}^2 \text{ s}^{-1}$ for stream function, and m s^{-1} for
7 wind vector.

8

9 Figure 13. Sketch of the physical processes linking the major summer monsoons in the NH and
10 the southern subtropical anticyclones. The three regions of rising motion, the three regions of
11 sinking motion and the regions of southern subtropical anticyclones affected are filled with gray,
12 sky blue and red colors, respectively. The sinking regions in the southeastern tropical Pacific and
13 the southeastern tropical Atlantic are indicated by sky blue borderlines. Thick black arrows
14 represent divergent winds in the upper level, while light green arrows represent the ray paths of
15 the stationary barotropic Rossby waves forced by diabatic cooling over the three regions of
16 sinking motion and by diabatic heating in the Indian summer monsoon region.

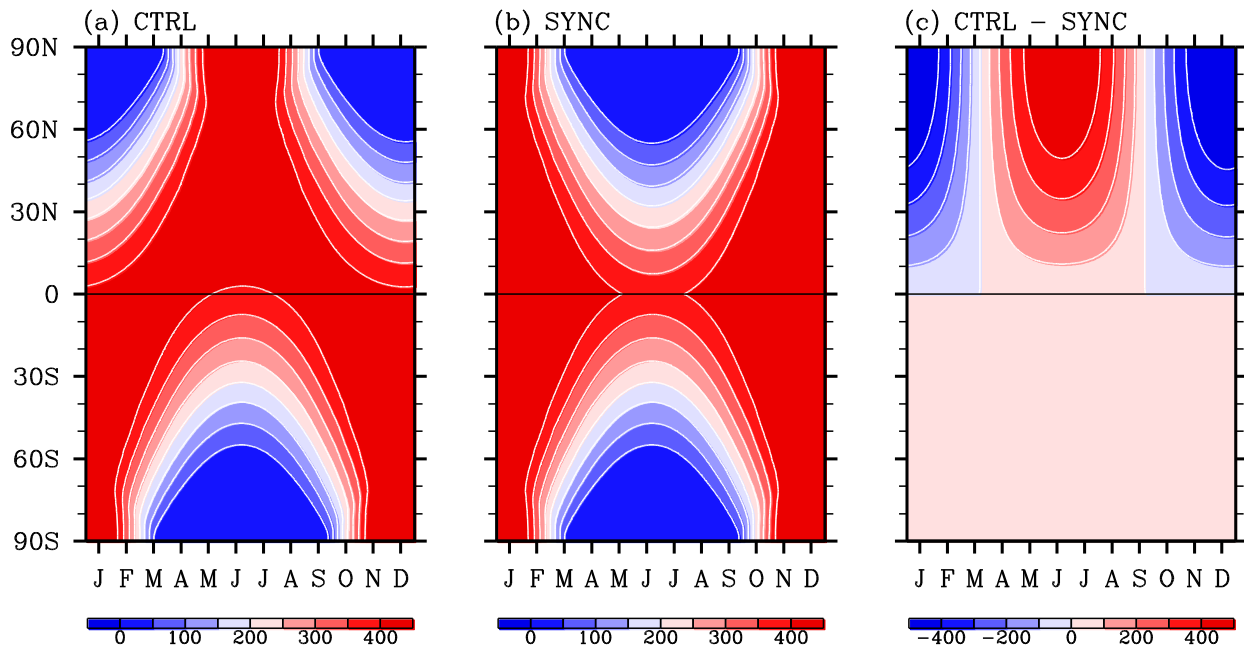
NCEP–NCAR Reanalysis: SLP



1
 2 Figure 1. Climatological sea level pressure for (a) DJF and (JJA) during 1971 - 2000 obtained
 3 from the NCEP-NCAR Reanalysis. The unit is hPa.

4
 5
 6
 7
 8
 9
 10
 11
 12
 13

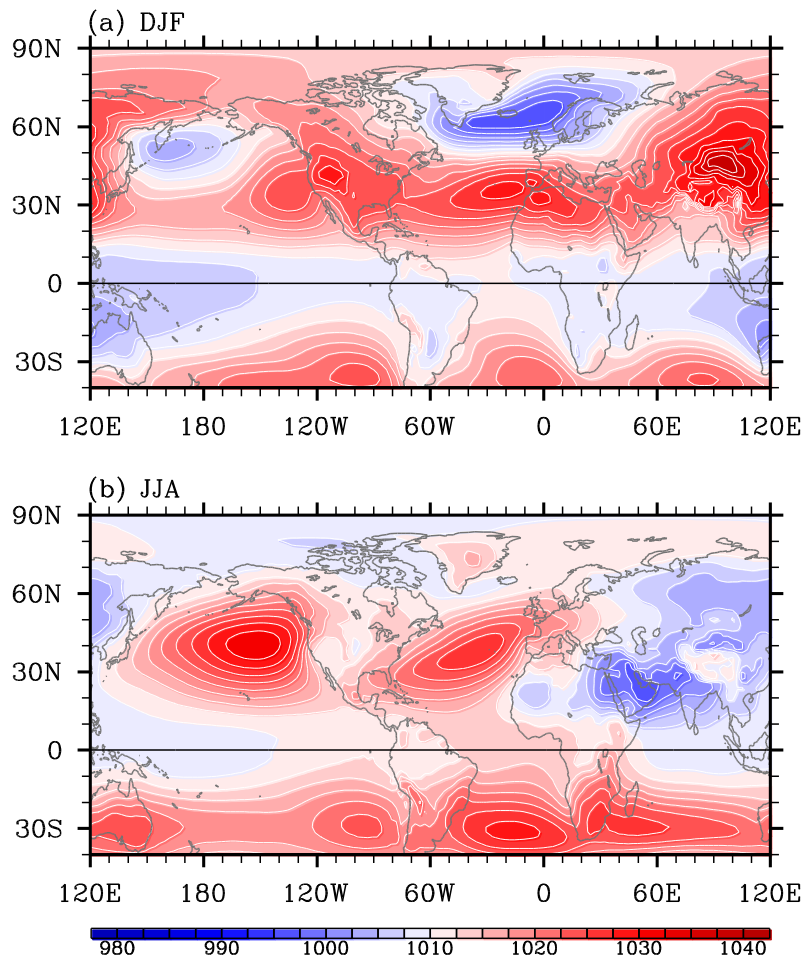
CAM4: TOA Solar Insolation



1
2
3
4
5
6
7
8
9
10
11
12
13
14
15
16
17
18
19

Figure 2. Daily solar insolation at the top of the atmosphere in (a) CTRL, and (b) SYNC, and (c) CTRL - SYNC. The unit is W m^{-2} .

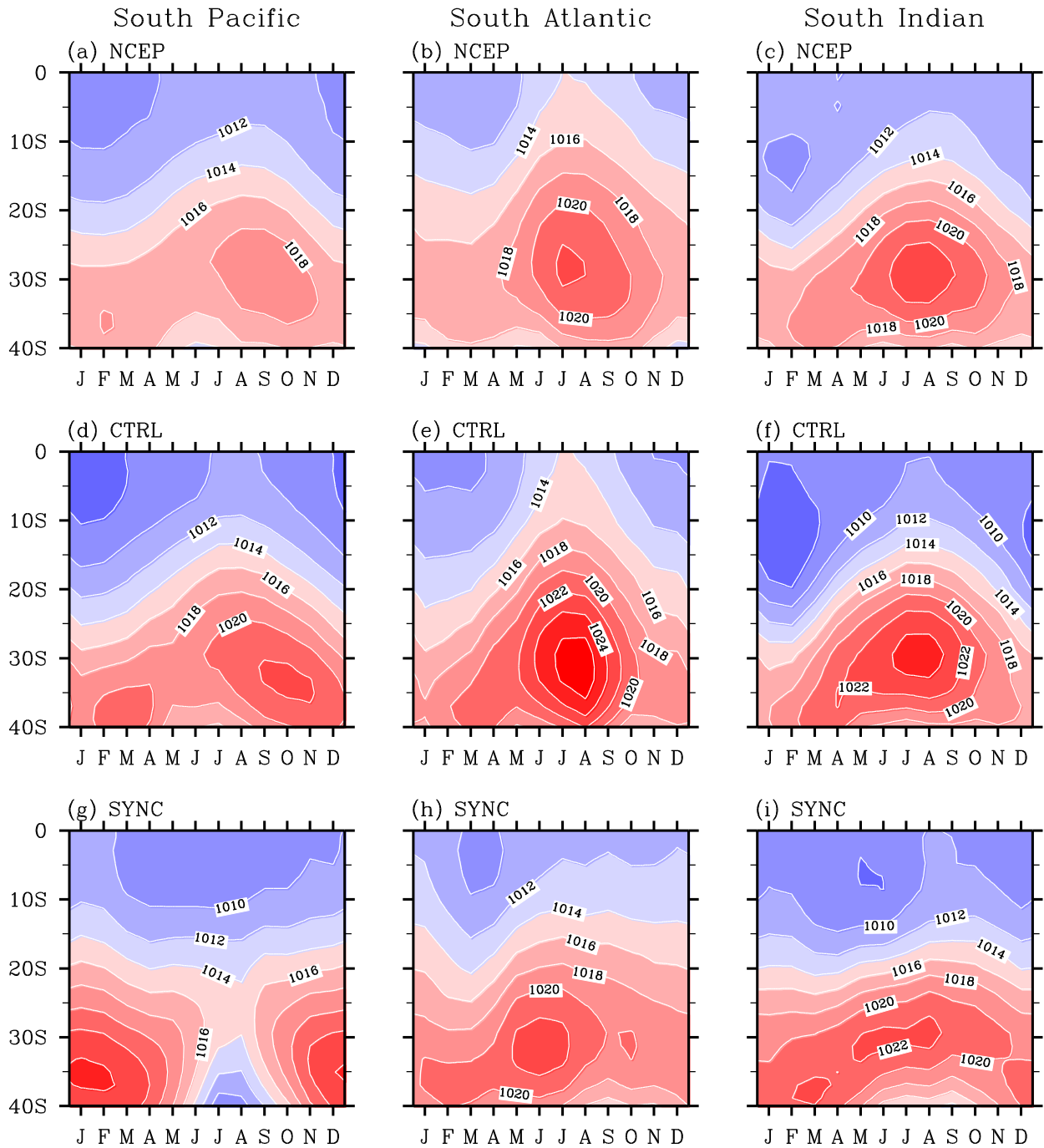
CAM4 (CTRL): SLP



1
2 Figure 3. Climatological sea level pressure for (a) DJF and (JJA) obtained from CTRL. The unit
3 is hPa.

4
5
6
7
8
9
10
11
12
13

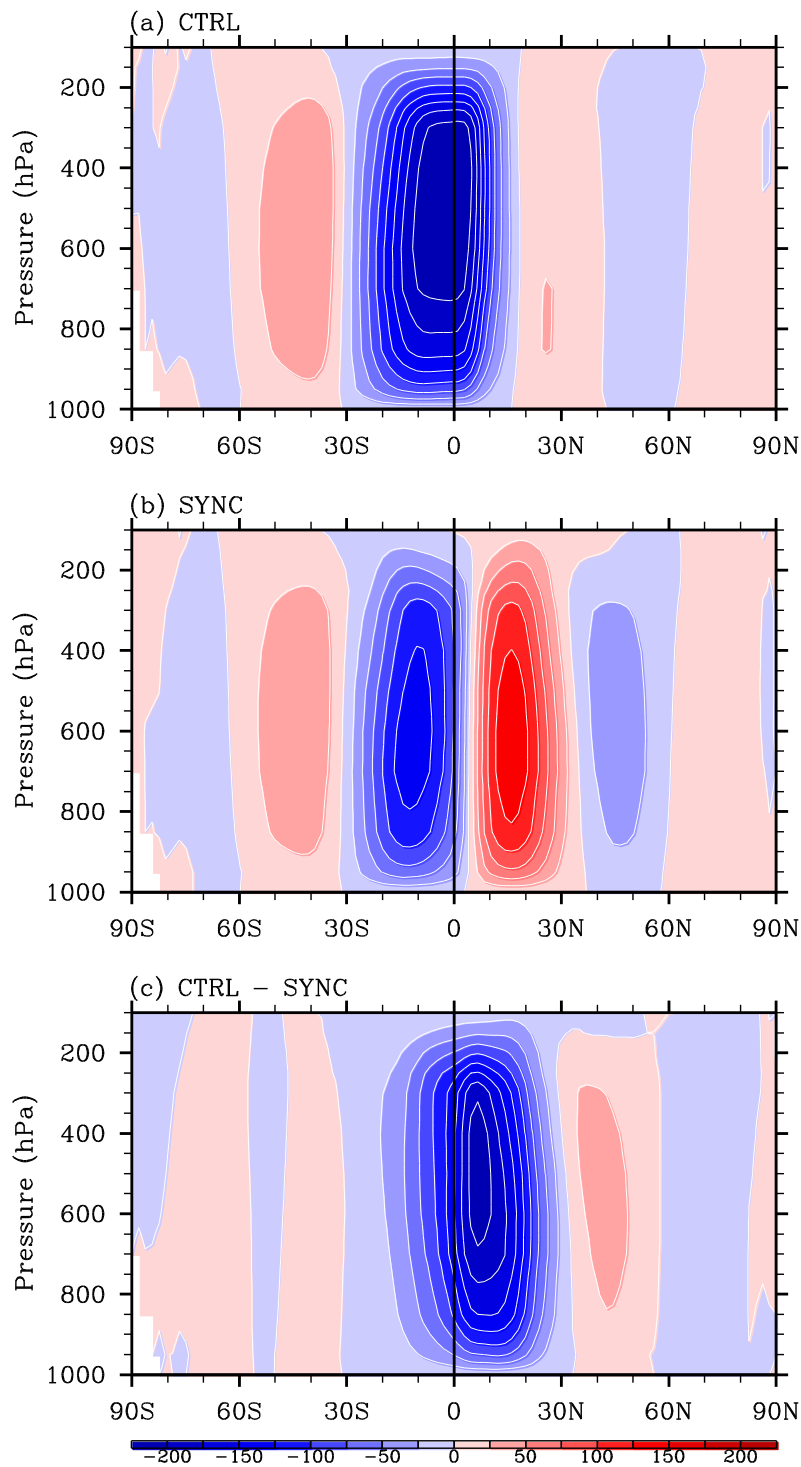
NCEP & CAM4: Zonally Averaged SLP for Each Ocean Basin



1
 2 Figure 4. Sea level pressure averaged zonally for (a, d, and g) the South Pacific Ocean, (b, e, and
 3 h) the South Atlantic Ocean, and (c, f, and i) South Indian Ocean, obtained from (a, b and c) the
 4 NCEP-NCAR reanalysis, (d, e and f) CTRL, and (g, h and i) SYNC. The unit is hPa.

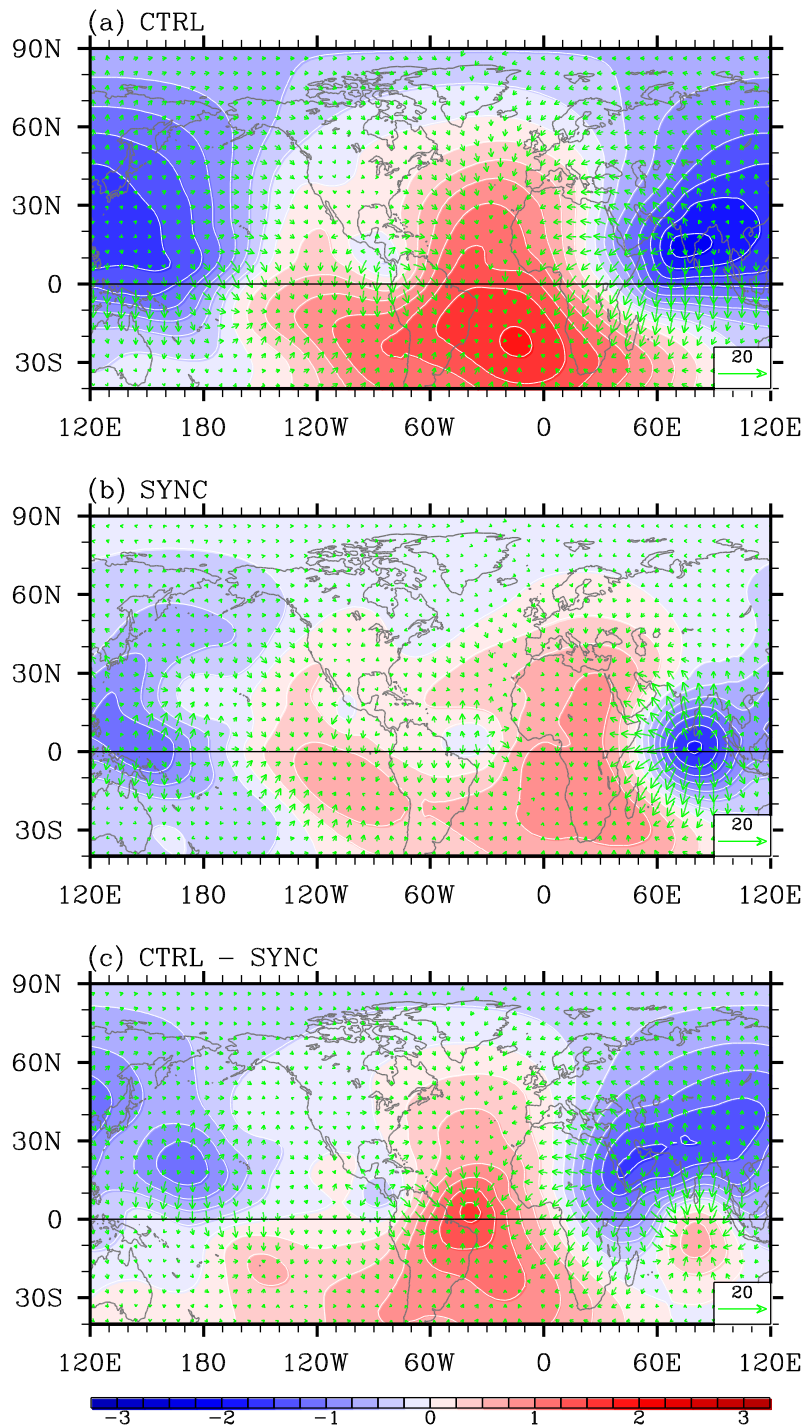
5
 6

CAM4: Hadley Circulation (JJA)



1
2 Figure 5. Meridional overturning circulation (mass stream function) obtained from (a) CTRL, (b)
3 SYNC, and (c) CTRL - SYNC. Circulation is clockwise (anticlockwise) around positive
4 (negative) stream function. The unit is 10^9 Kg s^{-1} .

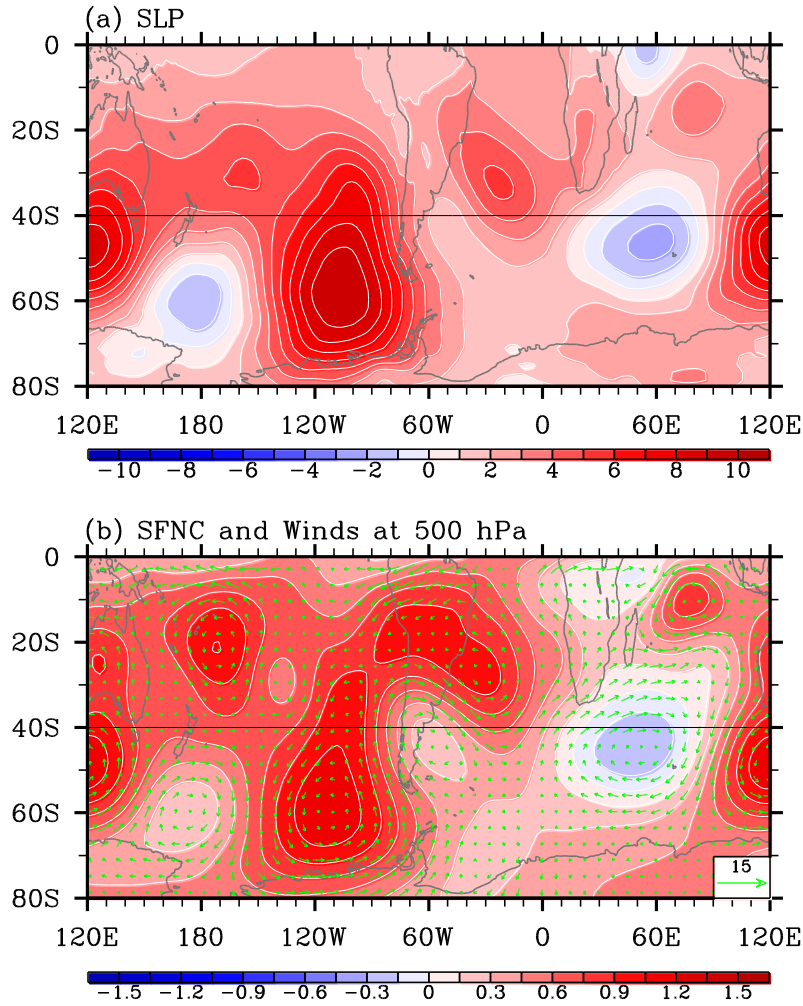
CAM4: VPOT & DIV Wind at 200hPa (JJA)



1
2 Figure 6. Velocity potential and divergent wind vector at 200 hPa obtained from (a) CTRL, (b)
3 SYNC, and (c) CTRL - SYNC. The units are $10^7 \text{ m}^2 \text{ s}^{-1}$ for velocity potential, and m s^{-1} for
4 divergent wind vector.

5

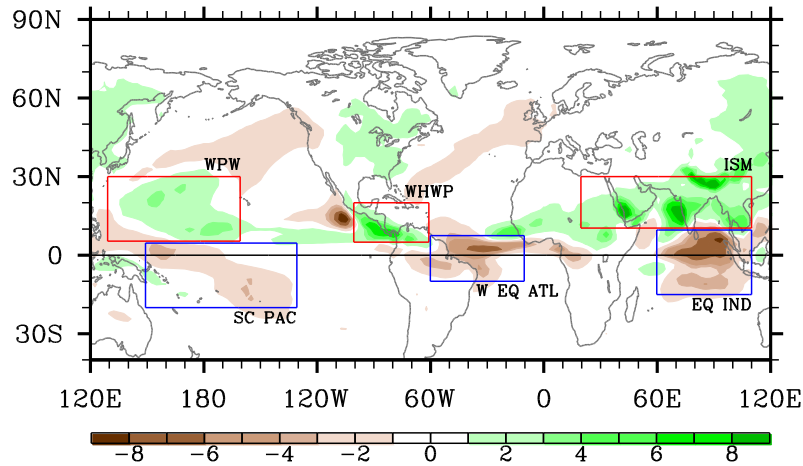
CAM4: CTRL - SYNC (JJA)



1
2 Figure 7. (a) Sea level pressure, (b) stream function and wind vector at 500 hPa obtained from
3 CTRL - SYNC. The zonal line at 40°S roughly marks the southern end of the southern
4 subtropical anticyclones in JJA. The stream function sign is reversed in such a way that
5 circulation is anticlockwise around positive stream function. The units are hPa for sea level
6 pressure, m for geopotential, and m s^{-1} for wind vector.

7
8
9
10
11
12

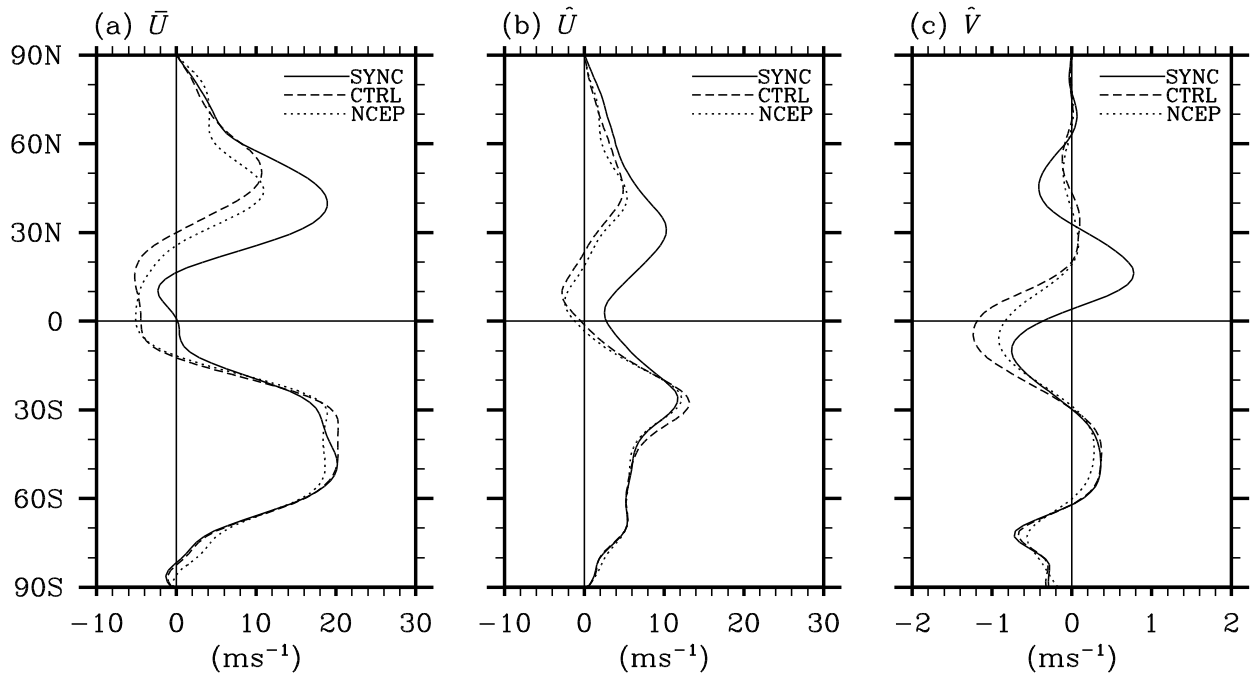
CAM4 (CTRL - SYNC): Conv. Heating (JJA)



1
2 Figure 8. Moist convective heating rate at 500 hPa in JJA obtained from CTRL - SYNC. The
3 three regions of diabatic heating in the NH, namely the northwestern Pacific Ocean affected by
4 summer expansion of the western Pacific warm pool, the WHWP, and the Indian summer
5 monsoon region are indicated by red borderlines. The three regions of diabatic cooling in the
6 equatorial oceans and the tropical SH, namely the south-central Pacific, the western equatorial
7 Atlantic, and the equatorial Indian Ocean are shown with blue borderlines. The unit is K day^{-1} .

8
9
10
11
12
13
14
15
16
17
18
19
20

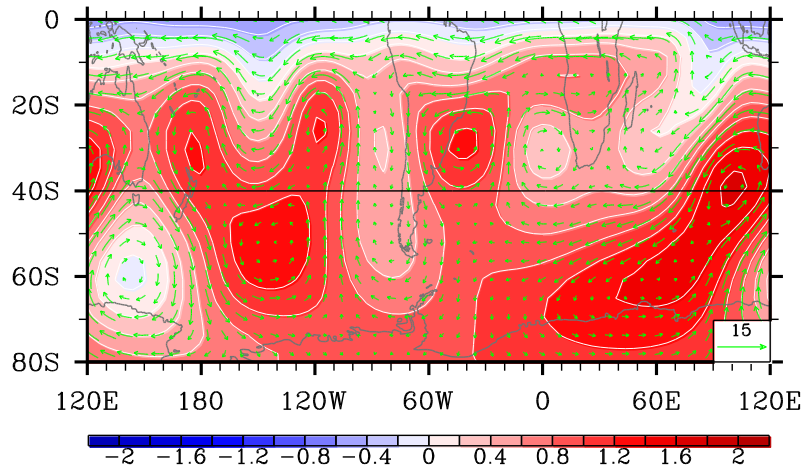
NCEP & CAM4: Background Flow (JJA)



1
 2 Figure 9. Zonally averaged climatological (a) barotropic zonal, (b) baroclinic zonal and (c)
 3 baroclinic meridional winds in JJA obtained from SYNC (solid lines), CTRL (long-dashed lines)
 4 and the NCEP-NCAR reanalysis (short-dashed line). The barotropic zonal winds are obtained by
 5 vertically averaging the zonal winds in the troposphere (100 ~ 1000 hPa). To compute the
 6 baroclinic zonal winds, the zonal winds are vertically averaged separately for the upper
 7 troposphere (100 ~ 500 hPa) and for the lower troposphere (500 ~ 1000 hPa), and the latter is
 8 subtracted from the former then divided by 2. The same methodology is used to compute the
 9 baroclinic meridional winds.

10
 11
 12
 13
 14
 15
 16
 17
 18

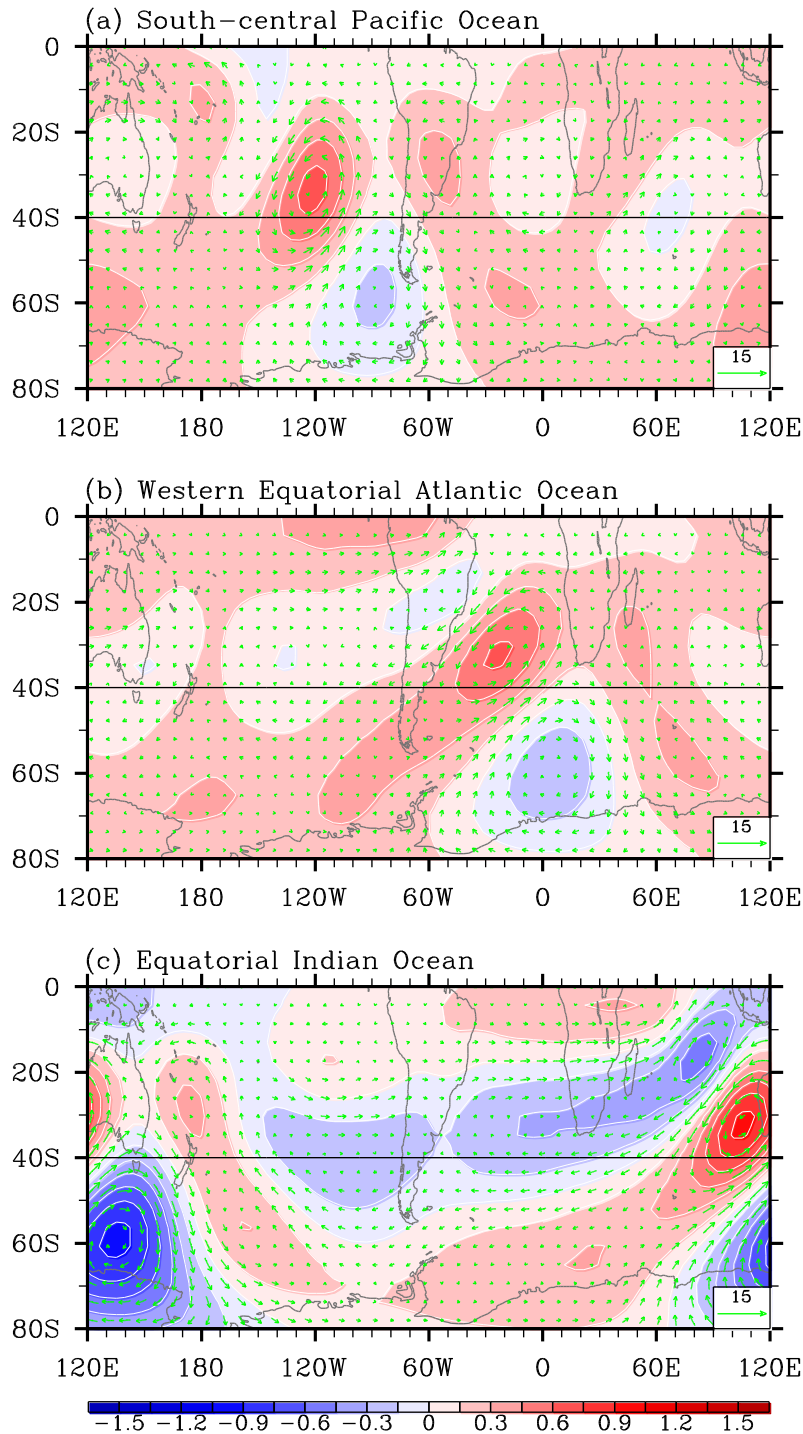
Simple Model: SFNC & Winds (JJA)



1
2
3
4
5
6
7
8
9
10
11
12
13
14
15
16
17
18
19
20
21
22

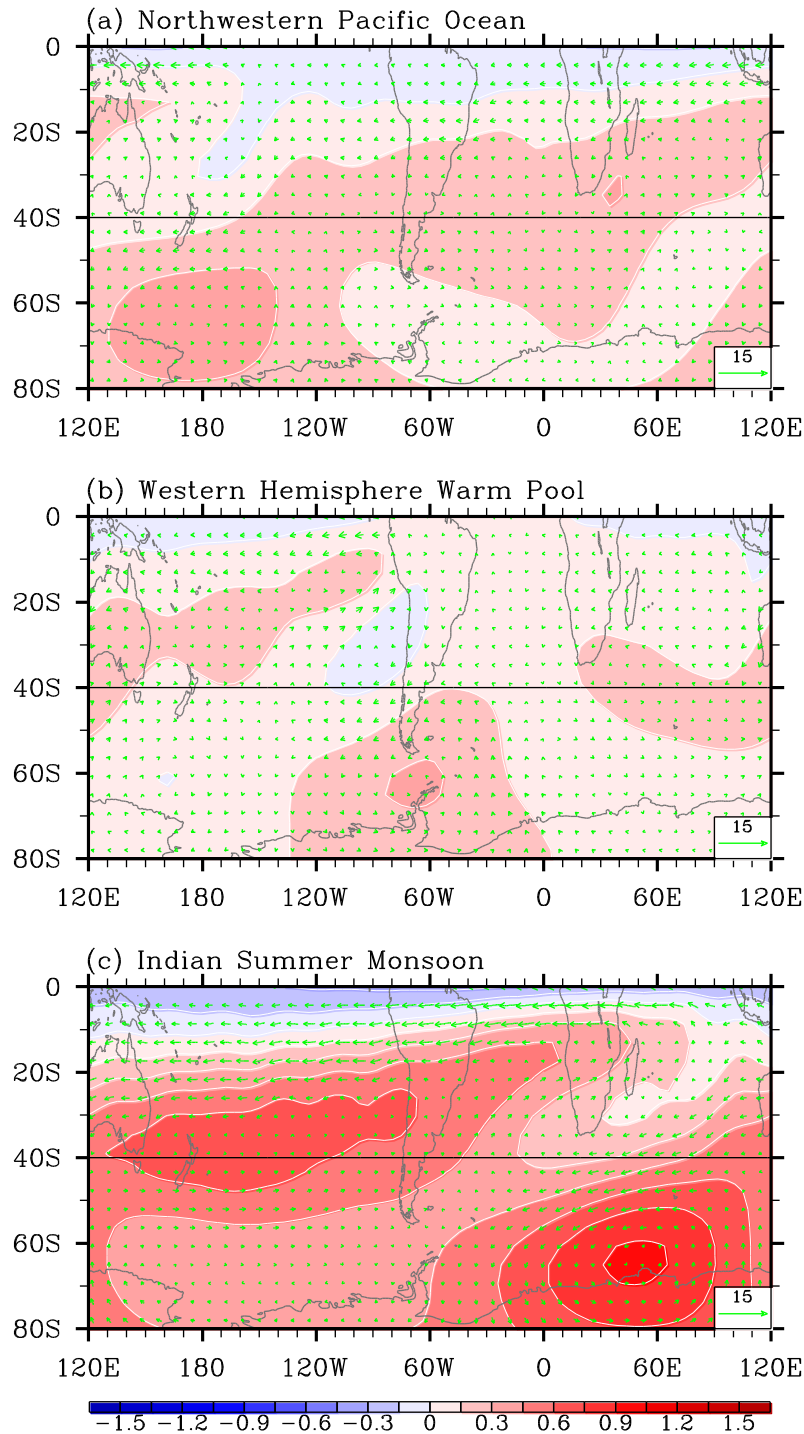
Figure 10. Barotropic stream function and wind vector responses in the simple model experiments to the moist convective heating and cooling derived from CTRL – SYNC. The units are $10^7 \text{ m}^2 \text{ s}^{-1}$ for stream function, and m s^{-1} for wind vector.

Simple Model: SFNC & Winds (JJA)

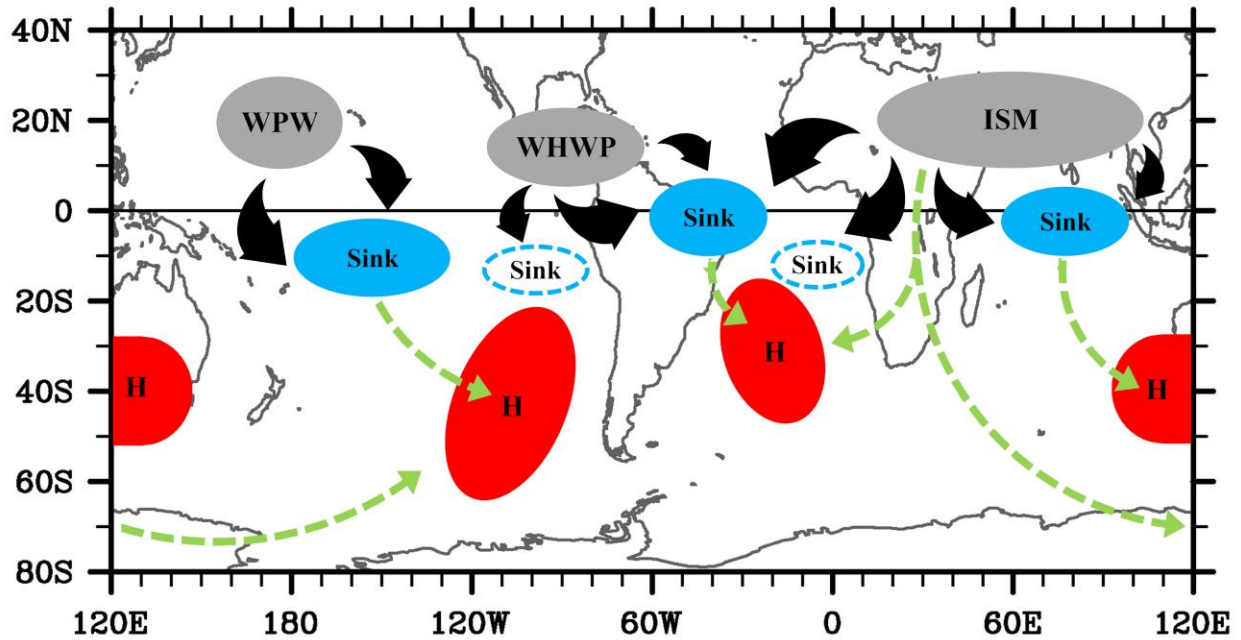


1
2 Figure 11. Barotropic stream function and wind vector responses in the simple model
3 experiments to diabatic cooling in (a) the central South Pacific Ocean, (b) the western equatorial
4 Atlantic Ocean, and (c) the equatorial Indian Ocean. The units are $10^7 \text{ m}^2 \text{ s}^{-1}$ for stream function,
5 and m s^{-1} for wind vector.

Simple Model: SFNC & Winds (JJA)



1
2 Figure 12. Barotropic stream function and wind vector responses in the simple model
3 experiments to diabatic cooling in (a) the northwestern Pacific Ocean, (b) the WHWP, and (c)
4 the Indian summer monsoon region. The units are $10^7 \text{ m}^2 \text{ s}^{-1}$ for stream function, and m s^{-1} for
5 wind vector.



1
 2 Figure 13. Sketch of the physical processes linking the major summer monsoons in the NH and
 3 the southern subtropical anticyclones. The three regions of rising motion, the three regions of
 4 sinking motion and the regions of southern subtropical anticyclones affected are filled with gray,
 5 sky blue and red colors, respectively. The sinking regions in the southeastern tropical Pacific and
 6 the southeastern tropical Atlantic are indicated by sky blue borderlines. Thick black arrows
 7 represent divergent winds in the upper level, while light green arrows represent the paths of the
 8 stationary barotropic Rossby waves forced by diabatic cooling over the three regions of sinking
 9 motion and by diabatic heating in the Indian summer monsoon region.